



**AFRL-RX-WP-JA-2019-0267**

**ELECTRON EMISSION CHARACTERISTICS OF WET  
SPUN CARBON NANOTUBE FIBERS (POSTPRINT)**

**T. C. Back, G. Gruen, J. Park, P. T. Murray, and S. B. Fairchild**

**AFRL/RXAN**

**J. Ludwick and M. Cahay**

**University of Cincinnati**

**29 May 2019  
Interim Report**

**DISTRIBUTION STATEMENT A.  
Approved for public release: distribution is unlimited.**

**© 2019 AUTHOR(S)**

**(STINFO COPY)**

**AIR FORCE RESEARCH LABORATORY  
MATERIALS AND MANUFACTURING DIRECTORATE  
WRIGHT-PATTERSON AIR FORCE BASE, OH 45433-7750  
AIR FORCE MATERIEL COMMAND  
UNITED STATES AIR FORCE**

# REPORT DOCUMENTATION PAGE

*Form Approved*  
OMB No. 0704-0188

The public reporting burden for this collection of information is estimated to average 1 hour per response, including the time for reviewing instructions, searching existing data sources, gathering and maintaining the data needed, and completing and reviewing the collection of information. Send comments regarding this burden estimate or any other aspect of this collection of information, including suggestions for reducing this burden, to Department of Defense, Washington Headquarters Services, Directorate for Information Operations and Reports (0704-0188), 1215 Jefferson Davis Highway, Suite 1204, Arlington, VA 22202-4302. Respondents should be aware that notwithstanding any other provision of law, no person shall be subject to any penalty for failing to comply with a collection of information if it does not display a currently valid OMB control number. **PLEASE DO NOT RETURN YOUR FORM TO THE ABOVE ADDRESS.**

<b>1. REPORT DATE (DD-MM-YY)</b> 29 May 2019		<b>2. REPORT TYPE</b> Interim		<b>3. DATES COVERED (From - To)</b> 29 October 2018 - 29 April 2019	
<b>4. TITLE AND SUBTITLE</b> Electron Emission Characteristics of Wet Spun Carbon Nanotube Fibers (Postprint)			<b>5a. CONTRACT NUMBER</b> In-House		
			<b>5b. GRANT NUMBER</b>		
			<b>5c. PROGRAM ELEMENT NUMBER</b>		
<b>6. AUTHOR(S)</b> T. C. Back, G. Gruen, J. Park, P. T. Murray, and S. B. Fairchild - AFRL/RXAN  (Continued on next page)			<b>5d. PROJECT NUMBER</b>		
			<b>5e. TASK NUMBER</b>		
			<b>5f. WORK UNIT NUMBER</b> X1SQ		
<b>7. PERFORMING ORGANIZATION NAME(S) AND ADDRESS(ES)</b> AFRL/RX 2977 Hobson Way Wright-Patterson AFB OH 45433  (Continued on next page)			<b>8. PERFORMING ORGANIZATION REPORT NUMBER</b>		
<b>9. SPONSORING/MONITORING AGENCY NAME(S) AND ADDRESS(ES)</b>  Air Force Research Laboratory Materials and Manufacturing Directorate Wright-Patterson Air Force Base, OH 45433-7750 Air Force Materiel Command United States Air Force			<b>10. SPONSORING/MONITORING AGENCY ACRONYM(S)</b> AFRL/RXAN		
			<b>11. SPONSORING/MONITORING AGENCY REPORT NUMBER(S)</b> AFRL-RX-WP-JA-2019-0267		
<b>12. DISTRIBUTION/AVAILABILITY STATEMENT</b> DISTRIBUTION STATEMENT A. Approved for public release: distribution is unlimited.					
<b>13. SUPPLEMENTARY NOTES</b> PA Case Number: 88ABW-2019-2326; Clearance Date: 29 May 2019. This document contains color. Journal article published in AIP Advances, Vol. 9, No. 6, 27 Jun 2019. © 2019 Author(s). The U.S. Government is joint author of the work and has the right to use, modify, reproduce, release, perform, display, or disclose the work. The final publication is available at <a href="https://doi.org/10.1063/1.5098328">https://doi.org/10.1063/1.5098328</a>					
<b>14. ABSTRACT (Maximum 200 words)</b> Wet spun carbon nanotube fibers were characterized using both field emission and electron energy distribution measurements. Fowler-Nordheim analysis of the field emission results showed that the carbon fibers demonstrated a large effective emission area, $2 \times 10^{-12} \text{ m}^2$ , which resulted in a reduced brightness of $1.84 \times 10^{10} \text{ A/m}^2/\text{sr/V}$ . By considering the emission and number of carbon nanotube emitters it can be shown that the brightness is consistent with previous reports for single nanotube emitters. Additionally, using the effective emission area determined from the Fowler-Nordheim analysis an emittance value around $0.70 \mu\text{m}$ was found. These characteristics are useful metrics in determining the applicability of using wet spun carbon nanotube fibers for field emission devices.					
<b>15. SUBJECT TERMS</b> Electron emission; Carbon nanotube fiber; Wet spun; Electron energy; Fowler-Nordheim analysis; Field emission; Emitters					
<b>16. SECURITY CLASSIFICATION OF:</b>			<b>17. LIMITATION OF ABSTRACT:</b> SAR	<b>18. NUMBER OF PAGES</b> 8	<b>19a. NAME OF RESPONSIBLE PERSON (Monitor)</b> Marc Martin <b>19b. TELEPHONE NUMBER (Include Area Code)</b> (937) 255-9645
<b>a. REPORT</b> Unclassified	<b>b. ABSTRACT</b> Unclassified	<b>c. THIS PAGE</b> Unclassified			

## REPORT DOCUMENTATION PAGE Cont'd

### 6. AUTHOR(S)

T. C. Back, G. Gruen, J. Park, P. T. Murray, and S. B. Fairchild - AFRL/RXAN

J. Ludwick and M. Cahay - University of Cincinnati

### 7. PERFORMING ORGANIZATION NAME(S) AND ADDRESS(ES)

AFRL/RX  
2977 Hobson Way  
Wright-Patterson AFB OH 45433

Spintronics and Vacuum Nanoelectronics Laboratory  
University of Cincinnati  
2600 Clifton Ave  
Cincinnati OH 45221

# Electron emission characteristics of wet spun carbon nanotube fibers

Cite as: AIP Advances 9, 065319 (2019); doi: 10.1063/1.5098328

Submitted: 1 April 2019 • Accepted: 20 June 2019 •

Published Online: 27 June 2019



View Online



Export Citation



CrossMark

T. C. Back,<sup>1,a)</sup> G. Gruen,<sup>1</sup> J. Park,<sup>1</sup> P. T. Murray,<sup>1</sup> J. Ludwick,<sup>2</sup> M. Cahay,<sup>2</sup> and S. B. Fairchild<sup>1</sup>

## AFFILIATIONS

<sup>1</sup>Materials and Manufacturing Directorate, Air Force Research Laboratory, WPAFB, Ohio 45433, USA

<sup>2</sup>Spintronics and Vacuum Nanoelectronics Laboratory, University of Cincinnati, Cincinnati, Ohio 45221, USA

<sup>a)</sup>Corresponding author: tyson.back.1@us.af.mil

## ABSTRACT

Wet spun carbon nanotube fibers were characterized using both field emission and electron energy distribution measurements. Fowler-Nordheim analysis of the field emission results showed that the carbon fibers demonstrated a large effective emission area,  $2 \times 10^{-12} \text{ m}^2$ , which resulted in a reduced brightness of  $1.84 \times 10^{10} \text{ A/m}^2/\text{sr/V}$ . By considering the emission and number of carbon nanotube emitters it can be shown that the brightness is consistent with previous reports for single nanotube emitters. Additionally, using the effective emission area determined from the Fowler-Nordheim analysis an emittance value around  $0.70 \mu\text{m}$  was found. These characteristics are useful metrics in determining the applicability of using wet spun carbon nanotube fibers for field emission devices.

© 2019 Author(s). All article content, except where otherwise noted, is licensed under a Creative Commons Attribution (CC BY) license (<http://creativecommons.org/licenses/by/4.0/>). <https://doi.org/10.1063/1.5098328>

New cathode options are needed to produce high current at low operating temperatures and for long time intervals. Because of their special electron-optical properties, high efficiency, fast response time, and resistance to radiation damage, as well as their portability and relatively simple nature, field electron emission (FE) cathodes offer a competitive and/or advantageous alternative to thermal emission cathodes for vacuum electronic applications. In particular, FE cold cathodes have received widespread attention, for applications including electron microscopy,<sup>1</sup> X-ray sources,<sup>2,3</sup> electronic devices,<sup>4,5</sup> terahertz sources,<sup>6,7</sup> and high-power microwave tubes.<sup>8,9</sup> Cathodes for these applications need to generate beams with good electron-optical properties, and to exhibit long lifetimes when subject to damaging conditions such as ion back-bombardment and intense heating.

Cold cathodes based on carbon nanotubes (CNTs) and carbon nanotube fibers (CNFs) have received considerable attention,<sup>10–18</sup> largely because of the high field enhancement brought about by their high aspect ratio and small apex radius, which facilitate emission at low applied voltages. CNTs are particularly attractive because they have excellent thermal and electrical conductivities which could potentially make them more robust to wide range operational conditions compared to traditional field emitter materials. Recently, wet spun carbon nanotube fiber(s)<sup>19</sup> (ws-CNF(s)) have been

experimentally shown to be capable of relatively high current densities,  $\sim 10^3 \text{ A/cm}^2$  at relatively low field strengths  $\sim 0.1\text{--}0.2 \text{ V}/\mu\text{m}$ . These enhanced FE properties have been shown to be related to the fairly high degree of alignment in ws-CNFs.<sup>20</sup> The ability to operate the FE cathode at high current densities and low field strength makes it possible to operate the cathode in wider range technologically relevant conditions. However, in order for the ws-CNFs to reach their full potential performance metrics such as field enhancement factors, current densities, brightness and emittance must be investigated in greater detail. Brightness and emittance are particularly important for electron microscopy and accelerator sources. Previously, most reported metrics deal with individual multi-walled or single-walled CNT emitters<sup>21,22</sup> The intent of this paper is to evaluate the field emission and electron energy distribution properties of ws-CNFs to determine their brightness and emittance.

Electron emission experiments were performed on CNFs made by the wet spinning technique. The wet spinning technique is described in detail elsewhere.<sup>19</sup> Fibers were mounted to a Mo sample holder held in place by Ag paste. The fiber was mounted in the vertical position, normal to the Mo plate surface. The length of the fiber from the sample holder surface to the fiber tip was 5 mm. Once the Ag was allowed to dry the sample was transferred into a surface analysis system with a prep and analysis chambers with a base

pressure of  $7 \times 10^{-10}$  and  $1 \times 10^{-10}$  Torr, respectively. FE measurements were carried out in the prep chamber. The sample was kept at ground with a positive bias on the anode of up to 1 keV. The anode tip consisted of stainless steel and was 3 mm in diameter. The gap distance between the anode and cathode was set at 5 mm using an optical camera and micrometers on the sample manipulator. FE experiments consisted of ramping the anode voltage in 1 V increments with 1 s dwell time. Current was measured at each voltage step with a Keithley 2600 source meter. Data acquisition was managed using LabView. Once the FE experiments were complete the sample was transferred into an analysis chamber for electron energy distribution (EED) measurements. These measurements were made by biasing the sample up to 500 eV with a Keithley 6487. The electron energy distribution and work function measurements were made with a hemispherical analyzer described elsewhere.<sup>23</sup> Consequently, the field strength and emission current for the FE and EED measurements were the same at  $0.05 \text{ V}/\mu\text{m}$  and  $\sim 70 \mu\text{A}$ , respectively. The EED measurement consisted of measuring the kinetic energy of field emitted electrons under these conditions by scanning near the applied bias on the sample. These measurements were made at a pass energy of 10 eV with 0.1 eV steps. Based on the hemispherical analyzer dimensions and gap distance we estimate the solid angle to be  $1.9 \times 10^{-6}$  sr.

Figure 1 shows SEM and Raman spectra from the ws-CNF. The morphology of the CNFs in the image is consistent with previously

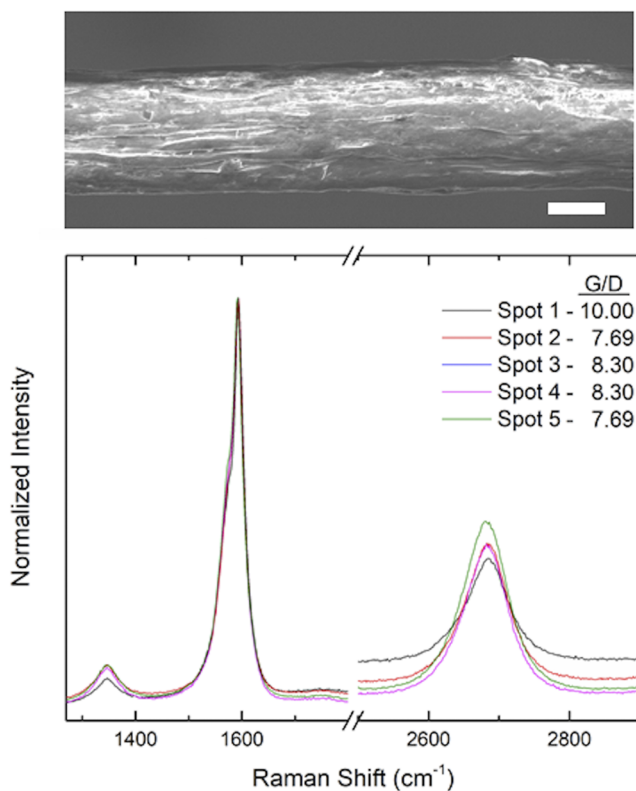


FIG. 1. Raman spectroscopy of CNT fiber. Spectra acquired along the length of the fiber yielding G/D ratio ranging 7-10. Scale bar is  $10 \mu\text{m}$ .

reported results of ws-CNFs.<sup>20</sup> The Raman spectra were acquired on the sidewall and tip of the fiber. There was no apparent difference between the tip and sidewall. A G/D ratio in the range of 7-10 was obtained from 5 different locations on the fiber. The G, D and 2D bands in the fiber were located at  $1593.9$ ,  $1347.0$  and  $2681.6 \text{ cm}^{-1}$ , respectively. Although higher G/D ratios have been obtained with ws-CNTs we note that the quality of the fibers were sufficient for FE experiments. We also note that the CNFs were not annealed or cleaned with solvent before FE experiments.

Figure 2 shows the results from the FE experiment. The ws-CNFs showed relatively smooth emission up to a 1000V. The maximum current shown in Figure 2 is well below the current levels where space charge and self-heating effects<sup>24,25</sup> become dominant. Consequently, we neglect any of these effects in the following analysis. The FE data was fit using the Fowler-Nordheim (FN) equation:

$$I(\text{Amps}) = a\beta_{\text{eff}}^2 E_{\text{ext}}^2 e^{-\frac{b}{\beta_{\text{eff}} E_{\text{ext}}}} (\text{A}/\text{m}^2), \quad (1)$$

where  $a = A_{\text{eff}} \frac{1.54 \times 10^{-6}}{\phi}$ ,  $b = 6.83 \times 10^9 \phi^{\frac{3}{2}}$ ,  $A_{\text{eff}}$  is the effective emission area,  $\phi$  is the CNF work function, and  $\beta_{\text{eff}}$  is the effective field enhancement factor. The FN fit shows slight underestimate of current around 600-900 V. We attribute this to adsorbate enhanced emission.<sup>26</sup> The inset in Figure 2 shows the FE current plotted in FN coordinates. A linear fit of the FN coordinates yielded a  $\beta_{\text{eff}}$  of  $5.57 \times 10^6$ . From the FN fit  $A_{\text{eff}}$  was calculated to be  $2.024 \times 10^{-12} \text{ m}^2$ . Tang *et al.* showed that using FN analysis to determine the emission area is a more accurate than using the physical dimensions of the emitter.<sup>27</sup> The effective emission area for the ws-CNFs are six orders of magnitude higher than what has been reported for a carbon fibers of the same dimension.<sup>27</sup> This is likely due to the geometry of the individual CNTs combined with the high degree of alignment within the fiber structure,<sup>20</sup> which results in a high density of emission sites.

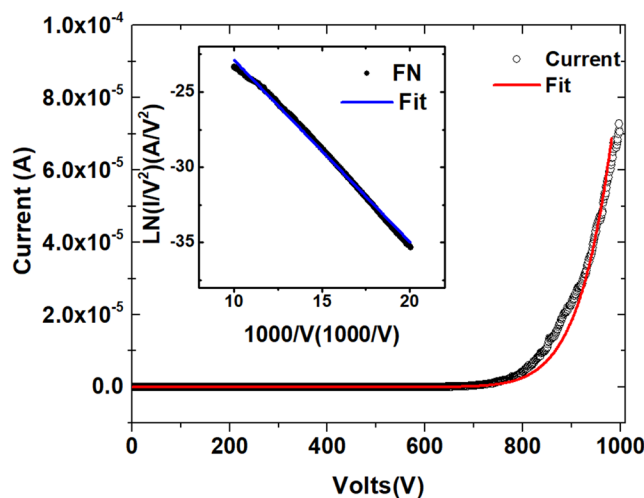
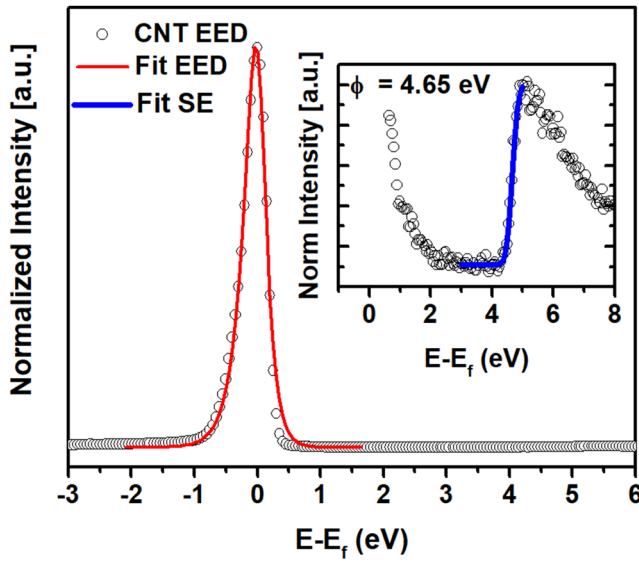


FIG. 2. Field emission results from carbon nanotube fibers. Inset shows field emission current plotted in FN coordinates. A linear fit to the FN coordinate data confirms field emission,  $R^2=0.99$ .



**FIG. 3.** Electron energy distribution of field emitted electrons. Fitted data (red) yielded a FWHM of 0.44 eV. Inset shows secondary emission onset caused by scattering of field emitted electrons from the fiber surface. The secondary emission onset was used to experimentally determine the work function of the CNT fiber,  $\Phi = 4.65$  eV. A brightness value of  $4.47 \times 10^7$  and a transverse energy of 0.25 eV was determined from the EED curve.

Once the FE experiments were completed, the sample was moved to the analysis chamber for EED measurements. Figure 3 shows the results of the EED measurement. The x-axis represents kinetic energy scale adjusted for the bias on the sample. All kinetic energies are referenced with respect to the Fermi level. The EED curve at zero binding energy is the result of field emitted electrons from the ws-CNFs. The field strength on the sample was set to match that of the FE experiment. The current measured on the sample under these conditions was  $\sim 70$   $\mu$ A identical to the FE experiment. The EED distribution can be approximated as follows<sup>28</sup>

$$J(E) = N \frac{\exp\left(\frac{E}{d}\right)}{1 + \exp\left(\frac{E}{kT}\right)}, \quad (2)$$

where  $N$  is a normalization constant and  $d$  is the mean transverse energy of the electron beam (eV). To accurately fit the distribution an additional instrumental Gaussian broadening term must be included in the form<sup>29</sup>

$$G_I = \frac{1}{\sigma\sqrt{2\pi}} \exp\left[-\frac{1}{2}\left(\frac{E}{\sigma}\right)^2\right], \quad (3)$$

where  $\sigma$  is the analyzer resolution. Results of the fit are shown in Figure 3. The FWHM of the distribution was determined to be 0.44 eV with a mean transverse energy ( $d$ ) of 0.25 eV, where the  $d$  is the energy spread on the low kinetic energy side of the EED curve measured from the Fermi level at half maximum. Once  $d$  is known, the reduced brightness  $B_r$  can be determined by the relationship<sup>21</sup>

$$B_r = \frac{I'}{\pi r_v^2 U}, \quad (4)$$

where  $r_v$  is the radius of the virtual source (m) and  $I'$  is the reduced emission current (A/sr). We assume that due to such a small solid angle,  $1.9 \times 10^{-6}$  sr, that  $r_v \cong r_p$ , where  $r_p$  is the physical source size.  $r_p$  is assumed to be equal to the effective emission area extracted from the Fowler Nordheim equation. Consequently, we use the effective emission area,  $2.024 \times 10^{-12}$  m<sup>2</sup>, as the physical source area.

The reduced brightness of the ws-CNT sample was found to be  $1.84 \times 10^{10}$  (A/m<sup>2</sup>/sr/V). This value is roughly an order of magnitude higher than the reduced brightness reported for a single CNT emitter,<sup>21</sup> which is in the range of  $1.3$ - $2.5 \times 10^9$  A/m<sup>2</sup>/sr/V.

The work function of the CNF can be extracted from the EED curves. The inset in Fig. 3 inset shows a blown up region of the EED spectrum where the secondary emission onset occurred for the ws-CNF sample. The secondary emission onset was fit with an error function<sup>30</sup> resulting in a work function  $\Phi$  of 4.65 eV. This is possible due to nanoscale roughness of the fiber surface and the fact that emission is not limited to the fiber tip.<sup>20,24</sup> Consequently, electrons going out into vacuum are inelastically scattered on the fiber surface causing secondary emission. A value of 4.65 eV is in reasonable agreement with tip emission reported elsewhere.<sup>31-34</sup> Being able to measure the work function experimentally eliminates some of the ambiguity linked with the extraction of the work function from Fowler Nordheim analysis.

An important measure of an electron beam quality is its emittance.<sup>35-37</sup> Emittance represents the volume occupied by the beam in phase space. An electron beam with a large degree of spreading will result in higher emittance. Consequently, characterizing the emittance of the beam extracted from a ws-CNF-based cathode is an important step in determining its usefulness for any desired application space. A commonly used form of emittance is normalized rms emittance,  $\epsilon_{n,rms}$ . The  $\epsilon_{n,rms}$  can be determined from the simple relationship  $\rho_c \sqrt{d}$ , where  $\rho_c$  is the square root of the effective emission area.<sup>38</sup> The  $\epsilon_{n,rms}$  of ws-CNFs was calculated to be 0.70  $\mu$ m. This value is similar to what has been found for photocathode sources used XFEL.<sup>38</sup>

Figure 4 shows a fit to the EED experimental data indicating a FWHM of 0.44 eV. The simulated spectrum was calculated by integrating the product of the transmission and supply functions described by<sup>39,40</sup>

$$J(F, T) = \frac{q}{2\pi\hbar} \int_0^\infty D(E)f(E)dE,$$

where  $D(E)$  denotes the transmission probability and  $f(E)$  denotes the electron supply function. This equation was evaluated numerically with work function, field strength and temperature as inputs. The work function and field strengths were set equal to 4.65 eV and 0.05 V/ $\mu$ m, respectively. In order to obtain a good fit with experimental data the temperature in the simulated current had to be adjusted to 778K (505  $^\circ$ C). This result suggests that, even at relatively low current densities, substantial Joule heating occurs through the emitting CNTs at the ws-CNF tip. In their model of resistive heating of a single CNT during FE, Purcell et al<sup>41</sup> calculated that the temperature at the tip of a 40  $\mu$ m long CNT with a 10nm radius and with a thermal conductivity  $\kappa$  of 100W/mK can reach a value as high as 1900K at an emission current of 2  $\mu$ A.

The temperature of 778K needed to fit the EED curve in Fig. 4 is an effective temperature which reflects the contribution from many CNTs emitting at the tip of the fiber. The CNTs with the largest

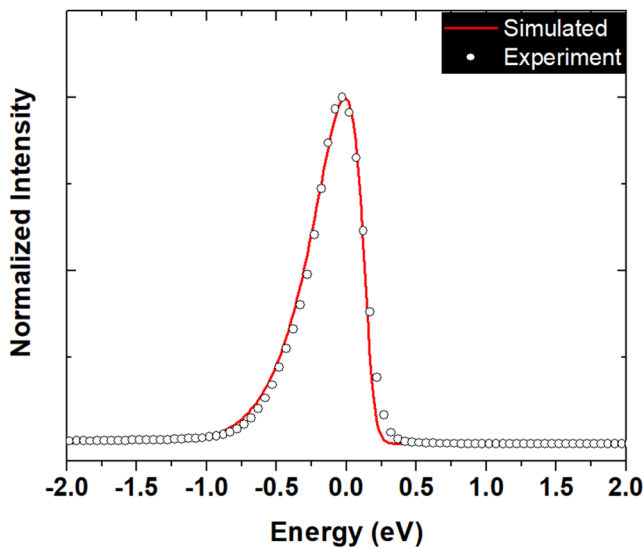


FIG. 4. Simulated field emission data (red) compared with experimental EED curve.

aspect ratio will predominantly determine the overall shape of the EED spectrum. Based on Purcell et al. calculations, a CNT tip temperature of 778 K is expected from a CNT with an emitting current of about  $0.7\mu\text{A}$ . Therefore, our measurements indicate that about 100 CNTs actively participate in the FE process and contribute to the EED spectrum shown in Fig. 4.

In summary, the reduced brightness and emittance of ws-CNFs have been determined to be  $1.84 \times 10^{10}$  and  $0.70 \mu\text{m}$ , respectively. The ws-CNFs have been shown to have an order of magnitude higher reduced brightness than previously reported. Electron energy distribution measurements suggested that the ws-CNFs had roughly 100 CNTs contributing to the total current. The emission characteristics of the ws-CNFs demonstrate improved performance over single nanotube emitters and offer a more robust solution to the environmental requirements of traditional FE emitters.

This material is based upon work supported by the Air Force Office of Scientific Research under award number FA9550-17RXCOR428.

## REFERENCES

- <sup>1</sup>H. Zhang, J. Tang, J. S. Yuan, Y. Yamauchi, T. T. Suzuki, N. Shinya, K. Nakajima, and L. C. Qin, *Nat. Nanotechnol.* **11**(3), 273 (2016).
- <sup>2</sup>M. T. Cole, R. J. Parmee, and W. I. Milne, *Nanotechnology* **27**(8), 082501 (2016).
- <sup>3</sup>C. Kottler, R. Longtin, S. Giudice, R. Jose-James, P. Niedermann, A. Neels, R. Kaufmann, J. R. Sanchez-Valencia, H. R. Elsener, O. Groning, C. Leinenbach, P. Groning, and A. Dommann, *Microelectron. Eng.* **122**, 13–19 (2014).
- <sup>4</sup>P. G. Collins and P. Avouris, *Sci. Am.* **283**(6), 62 (2000).
- <sup>5</sup>R. Rao, C. L. Pint, A. E. Islam, R. S. Weatherup, S. Hofmann, E. R. Meshot, F. Q. Wu, C. W. Zhou, N. Dee, P. B. Amama, J. Carpena-Nunez, W. B. Shi, D. L. Plata, E. S. Penev, B. I. Yakobson, P. B. Balbuena, C. Bichara, D. N. Futaba, S. Noda, H. M. Shin, K. S. Kim, B. Simard, F. Mirri, M. Pasquali, F. Fornasiero, E. I. Kauppinen, M. Arnold, B. A. Cola, P. Nikolaev, S. Arepalli, H. M. Cheng, D. N. Zakharov, E. A. Stach, J. Zhang, F. Wei, M. Terrones, D. B. Geohegan, B. Maruyama, S. Maruyama, Y. Li, W. W. Adams, and A. J. Hart, *ACS Nano* **12**(12), 11756–11784 (2018).

- <sup>6</sup>J. H. Booske, *Phys. Plasmas* **15**(5), 055502 (2008).
- <sup>7</sup>J. H. Booske, R. J. Dobbs, C. D. Joye, C. L. Kory, G. R. Neil, G. S. Park, J. Park, and R. J. Temkin, *IEEE Trans. Terahertz Sci. Technol.* **1**(1), 54–75 (2011).
- <sup>8</sup>D. Shiffler, M. Haworth, K. Cartwright, R. Umstaddt, M. Ruebush, S. Heidger, M. LaCour, K. Golby, D. Sullivan, P. Duselis, and J. Luginsland, *IEEE Trans. Plasma Sci.* **36**(3), 718–728 (2008).
- <sup>9</sup>D. Shiffler, M. Ruebush, M. Haworth, R. Umstaddt, M. LaCour, K. Golby, D. Zagar, and T. Knowles, *Rev. Sci. Instrum.* **73**(12), 4358–4362 (2002).
- <sup>10</sup>M. Cahay, W. Zhu, J. Ludwick, K. L. Jensen, R. G. Forbes, S. B. Fairchild, T. C. Back, P. T. Murray, J. R. Harris, and D. A. Shiffler, in *Nanotube Superfiber Materials, Science, Manufacturing and Commercialization*, edited by M. Schulz, V. Shanov, Z. Yin, and M. Cahay (Elsevier, 2019).
- <sup>11</sup>W. Zhu, M. Cahay, J. Ludwick, K. L. Jensen, R. G. Forbes, S. B. Fairchild, T. C. Back, P. T. Murray, J. R. Harris, and D. A. Shiffler, edited by M. Schulz, V. Shanov, Z. Yin, and M. Cahay (Elsevier, 2019).
- <sup>12</sup>G. S. Bocharov and A. V. Eletsii, *Nanomaterials* **3**(3), 393–442 (2013).
- <sup>13</sup>J. M. Bonard, M. Croci, C. Klinke, R. Kurt, O. Noury, and N. Weiss, *Carbon* **40**(10), 1715–1728 (2002).
- <sup>14</sup>J. M. Bonard, H. Kind, T. Stockli, and L. A. Nilsson, *Solid-State Electron.* **45**(6), 893–914 (2001).
- <sup>15</sup>J. M. Bonard, J. P. Salvetat, T. Stockli, W. A. de Heer, L. Forro, and A. Chatelain, *Applied Physics Letters* **73**(7), 918–920 (1998).
- <sup>16</sup>X. Calderon-Colon, H. Z. Geng, B. Gao, L. An, G. H. Cao, and O. Zhou, *Nanotechnology* **20**(32), 325707 (2009).
- <sup>17</sup>N. de Jonge, Y. Lamy, K. Schoots, and T. H. Oosterkamp, *Nature* **420**(6914), 393–395 (2002).
- <sup>18</sup>M. F. L. de Volder, S. H. Tawfick, R. H. Baughman, and A. J. Hart, *Science* **339**(6119), 535–539 (2013).
- <sup>19</sup>N. Behabtu, C. C. Young, D. E. Tsentlovich, O. Kleinerman, X. Wang, A. W. K. Ma, E. A. Bengio, R. F. ter Waarbeek, J. J. de Jong, R. E. Hoogerwerf, S. B. Fairchild, J. B. Ferguson, B. Maruyama, J. Kono, Y. Talmon, Y. Cohen, M. J. Otto, and M. Pasquali, *Science* **339**(6116), 182–186 (2013).
- <sup>20</sup>S. B. Fairchild, J. Boeckl, T. C. Back, J. B. Ferguson, H. Koerner, P. T. Murray, B. Maruyama, M. A. Lange, M. M. Cahay, N. Behabtu, C. C. Young, M. Pasquali, N. P. Lockwood, K. L. Averett, G. Gruen, and D. E. Tsentlovich, *Nanotechnology* **26**(10), 105706 (2015).
- <sup>21</sup>N. de Jonge, *J. Appl. Phys.* **95**(2), 673–681 (2004).
- <sup>22</sup>N. de Jonge, in *Advances in Imaging and Electron Physics*, Vol. 156, edited by P. W. Hawkes (Elsevier Academic Press Inc, San Diego, 2009), Vol. 156, pp. 203–233.
- <sup>23</sup>S. B. Fairchild, P. Zhang, J. Park, T. C. Back, D. Marincel, Z. Huang, and M. Pasquali, *IEEE Trans. Plasma Sci.* **47**, 2032 (2019).
- <sup>24</sup>M. Cahay, P. T. Murray, T. C. Back, S. Fairchild, J. Boeckl, J. Bulmer, K. K. K. Koziol, G. Gruen, M. Sparkes, F. Orozco, and W. O'Neill, *Applied Physics Letters* **105**(17), 173107 (2014).
- <sup>25</sup>M. Cahay, W. Zhu, S. Fairchild, P. T. Murray, T. C. Back, and G. J. Gruen, *Applied Physics Letters* **108**(3), 033110 (2016).
- <sup>26</sup>P. T. Murray, T. C. Back, M. M. Cahay, S. B. Fairchild, B. Maruyama, N. P. Lockwood, and M. Pasquali, *Applied Physics Letters* **103**(5), 053113 (2013).
- <sup>27</sup>W. W. Tang, D. A. Shiffler, J. R. Harris, K. L. Jensen, K. Golby, M. LaCour, and T. Knowles, *AIP Adv.* **6**(9), 095007 (2016).
- <sup>28</sup>N. de Jonge, M. Alliou, M. Doytcheva, M. Kaiser, K. B. K. Teo, R. G. Lacerda, and W. I. Milne, *Applied Physics Letters* **85**(9), 1607–1609 (2004).
- <sup>29</sup>R. Reifenger, H. A. Goldberg, and M. J. G. Lee, *Surf. Sci.* **83**(2), 599–616 (1979).
- <sup>30</sup>C. Mathieu, N. Barrett, J. Rault, Y. Y. Mi, B. Zhang, W. A. de Heer, C. Berger, E. H. Conrad, and O. Renault, *Physical Review B* **83**(23), 235436 (2011).
- <sup>31</sup>S. Suzuki, C. Bower, T. Kiyokura, K. G. Nath, Y. Watanabe, and O. Zhou, *Journal of Electron Spectroscopy and Related Phenomena* **114–116**, 225–228 (2001).
- <sup>32</sup>S. Suzuki, Y. Watanabe, Y. Homma, S.-y. Fukuba, S. Heun, and A. Locatelli, *Applied Physics Letters* **85**(1), 127–129 (2004).
- <sup>33</sup>C. J. Edgcombe and N. de Jonge, *Journal of Physics D: Applied Physics* **40**(14), 4123–4128 (2007).

- <sup>34</sup>Z. Xu, X. D. Bai, E. G. Wang, and Z. L. Wang, [Applied Physics Letters](#) **87**(16), 163106 (2005).
- <sup>35</sup>K. L. Jensen, P. G. O'Shea, and D. W. Feldman, [Phys. Rev. Spec. Top.-Accel. Beams](#) **13**(8), 080704 (2010).
- <sup>36</sup>K. L. Jensen, P. G. O'Shea, D. W. Feldman, and J. L. Shaw, [J. Appl. Phys.](#) **107**(1), 014903 (2010).
- <sup>37</sup>K. L. Jensen, D. A. Shiffler, J. J. Petillo, Z. G. Pan, and J. W. Luginsland, [Phys. Rev. Spec. Top.-Accel. Beams](#) **17**(4), 043402 (2014).
- <sup>38</sup>N. A. Moody, K. L. Jensen, A. Shabaev, S. G. Lambrakos, J. Smedley, D. Finkenstadt, J. M. Pietryga, P. M. Anisimov, V. Pavlenko, E. R. Batista, J. W. Lewellen, F. Liu, G. Gupta, A. Mohite, H. Yamaguchi, M. A. Hoffbauer, and I. Robel, [Physical Review Applied](#) **10**(4), 047002 (2018).
- <sup>39</sup>K. L. Jensen and M. Cahay, [Applied Physics Letters](#) **88**(15), 154105 (2006).
- <sup>40</sup>E. L. Murphy and R. H. Good, [Physical Review](#) **102**(6), 1464–1473 (1956).
- <sup>41</sup>S. T. Purcell, P. Vincent, C. Journet, and V. T. Binh, [Physical Review Letters](#) **88**(10), 105502 (2002).